(Received 3 October 2025, Accepted 11 November 2025, Scheduled 4 December 2025)

CPW- and MSL-to-RWG TE_{20} Mode Transitions

Yueh-Hsien Cheng and Chun-Long Wang*

National Taiwan University of Science and Technology, Taipei 106335, Taiwan

ABSTRACT: In this paper, a coplanar waveguide-to-rectangular waveguide TE_{20} mode transition using an antisymmetric tapered probe is proposed. The transmission coefficient of the TE_{20} mode is nearly 0 dB, and the reflection coefficient of the coplanar waveguide mode is smaller than −10 dB from 13.48 GHz to 14.7 GHz. In this frequency range, the transmission coefficient of the TE_{10} mode is smaller than −20 dB while the reflection coefficient of the coupled slotline mode is smaller than −19 dB. Besides, a microstrip line-to-rectangular waveguide TE_{20} mode transition using an antisymmetric fork is proposed. The transmission coefficient of the TE_{20} mode is nearly 0 dB, and the reflection coefficient of the microstrip line mode is smaller than −10 dB from 13.34 GHz to 15 GHz. In this frequency range, the transmission coefficient of the TE_{10} mode is smaller than −20 dB. To verify simulation results, the coplanar waveguide-to-rectangular waveguide TE_{20} transition and microstrip line-to-rectangular waveguide TE_{20} mode transition are back-to-back fabricated and measured, with the measurement results agreeing well with the simulation ones.

1. INTRODUCTION

The early development of microwave circuits was mainly based on waveguide structures such as coaxial cables and rectangular waveguides. Due to the characteristics of low loss and high-power carrying capacity, rectangular waveguides are widely used in long-distance transmission systems such as radar satellite communications, military, and aerospace communications. In the 1960s, planar transmission lines emerged, making microwave circuits diverse. Planar transmission lines have a variety of structures, such as microstrip lines, coplanar waveguides, coplanar strip lines, and slotlines. These structures have characteristics of small size, low price, easy making, and easy integrating with monolithic microwave integrated circuits or microwave integrated circuits. Therefore, they have been widely used in the design of microwave components in recent years. Among these planar transmission lines, microstrip lines and coplanar waveguides are easier to achieve low characteristic impedance, so they are more commonly used. In order to integrate planar circuit components and rectangular waveguide components, a transition from planar transmission lines to rectangular waveguides is required.

Many scholars have proposed various types of coplanar waveguide-to-rectangular waveguide TE_{10} mode transitions [1–9]. First, in 1990, a coplanar waveguide-to-rectangular waveguide TE_{10} mode transition using a ridge waveguide was proposed by Ponchak and Simons [1]. Although this transition has a broadband response and extremely low loss, the transition uses a ridge waveguide to achieve field matching, which is difficult to process, expensive, and bulky. In 2009, Shireen et al. applied ridge waveguide to the W-band [2]. Although this transition can achieve a broadband response, it was also bulky and difficult to process.

In order to solve the problems of large size, inconvenience to carry, and difficulty in processing, some scholars directly fabricated transition on substrate [3–9]. First, a coplanar waveguide-to-rectangular waveguide TE_{10} mode transition using a dipole slot antenna was proposed [3]. This structure is extremely simple, using only a quarter wavelength for impedance matching, but the bandwidth of this transition is not very wide. In order to further reduce the area of the transition, some scholars use extremely small slot antennas to achieve the transition from coplanar waveguide to rectangular waveguide [4]. Although the area of this transition circuit is quite small, a quarter-wavelength short-circuited waveguide is required in the back direction, which occupies the transition volume.

In order to increase the bandwidth, some scholars use conical fin-lines to excite the TE_{10} mode of the rectangular waveguide [5]. This transition circuit is easy to manufacture, has a wideband frequency response, and is suitable for high and low dielectric constant substrates. However, using conical fin-lines to gradually match the field pattern and impedance to the rectangular waveguide requires a large area. In order to reduce the area, some scholars proposed a conical slotline probe structure to excite the TE_{10} mode of the rectangular waveguide [6]. Although this structure can achieve a wideband frequency response and slightly reduce the transition area, this structure still requires a relay switch to achieve the overall transition, so its circuit area reduction is limited. In addition, some scholars use a simple probe structure to match the field pattern to rectangular waveguide TE_{10} mode [7]. Although the probe structure only needs a quarter wavelength, another quarter-wavelength substrate is required at its end to achieve a broadband transition design, so the area reduction is limited. To eliminate the substrate at the end, a coplanar waveguide-to-rectangular waveguide TE_{10} mode transition utilizing an inductor-compensated slotline was developed [8]. This transition uses an inductor-

* Corresponding author: Chun-Long Wang (clw@mail.ntust.edu.tw).

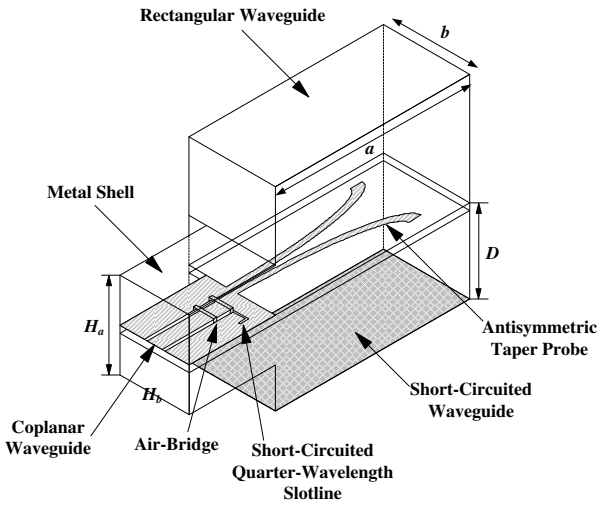

FIGURE 1. The schematic view of the coplanar waveguide-to-rectangular waveguide TE_{20} mode transition using the antisymmetric tapered probe.

compensated slotline to shrink the quarter-wavelength slotline and integrate it into the bow-tie transition to save circuit area. Some scholars further reduced the inductor-compensated slotline by using a 90° resonator to accomplish the transition [9].

The TE_{20} mode of rectangular waveguides is becoming increasingly important today as it has been used in the design of antennas [10–12] and filters [13]. As for high-order modes rectangular waveguide transitions, a variety of transitions are also proposed [14–17]. Some scholars have used curved rectangular waveguide bends to design a rectangular waveguide TE_{10} mode to TE_{20} mode or TE_{40} mode transitions [14]. By using one rectangular waveguide bend, a broadband rectangular waveguide TE_{10} mode to TE_{20} mode transition can be accomplished. By utilizing two rectangular waveguide bends, a broadband rectangular waveguide TE_{10} mode to TE_{40} mode transition can be accomplished. Although this transition can achieve a broadband response, it occupies an extremely large volume. In addition, in 2016, some scholars proposed a rectangular waveguide TE_{10} mode to cylindrical waveguide TE_{13} mode transition [15]. This structure first converts rectangular waveguide TE_{10} mode to TE_{50} mode through a front-end transition, and then converts the TE_{50} mode to cylindrical waveguide TE_{13} mode. The transition is broadband and can reduce the transition volume of the rectangular waveguide. However, the fabrication process of this transition is quite complicated, and the volume is still large. In addition, some scholars use similar transitions at the front end to convert rectangular waveguide TE_{10} mode into rectangular waveguide TE_{n0} mode, and then convert the TE_{n0} mode into different cylindrical waveguide modes [16]. Although the transition is broadband, the fabrication process is also complicated, and the transition still occupies a large volume. To reduce the volume, some scholars use two fin-line structures to convert rectangular waveguide TE_{10} mode to rectangular waveguide TE_{20} mode [17]. Although the transition volume can be greatly reduced, the transition bandwidth is very narrow. As two fin-line structures with a phase difference of 180° are required, the transition still occupies a substantial volume. To further reduce the transition volume, a miniaturized coplanar waveguide-to-rectangular waveguide TE_{20} mode transition using an antisymmetric tapered probe is proposed. As there will be TE_{10} mode and TE_{20} mode propagating in the rectangular waveguide at the same time, the antisymmetric tapered probe should be properly designed so that there will be solely TE_{20} mode propagating in the rectangular waveguide without TE_{10} mode propagating in the rectangular waveguide, and the transition can maintain a compact size. In addition, a miniaturized microstrip line-to-rectangular waveguide TE_{20} mode transition using an antisymmetric fork is proposed. For the same reason, the antisymmetric fork should be properly designed so that there will be solely TE_{20} mode propagating in the rectangular waveguide without TE_{10} mode propagating in the rectangular waveguide, and the transition can maintain a compact size.

2. COPLANAR WAVEGUIDE-TO-RECTANGULAR WAVEGUIDE TE_{20} MODE TRANSITION USING ANTISYMMETRIC TAPERED PROBE

2.1. Topology

The schematic view of the coplanar waveguide-to-rectangular waveguide TE_{20} mode transition using an antisymmetric tapered probe is shown in Figure 1, and its planar circuit is shown in Figure 2. The substrate used for the planar circuit is Rogers®RO5880, with a dielectric constant of 2.2, a tangent loss of 0.0009, and a substrate thickness of 0.8 mm. From the planar circuit in Figure 2, the 75-Ω coplanar waveguide is fed into the front end of the circuit. One slot of the coplanar waveguide is terminated with a short-circuited quarter-wavelength slotline, and the other slot is fed into the coplanar stripline and antisymmetric tapered probe. The coplanar stripline and antisymmetric tapered probe are used to gradually match the field pattern and impedance to the rectangular waveguide TE_{20} mode. The rectangular waveguide used is rectangular waveguide WR-90 ($a = 22.86\,\text{mm} \times b = 10.16\,\text{mm}$). The cutoff frequency of TE_{10} mode is 6.56 GHz; the cutoff frequency of TE_{20} mode is 13.1 GHz; the cutoff frequency of TE_{01} mode is 14.76 GHz. As a result, the operating frequency band of TE_{20} mode is between the cutoff frequency of TE_{20} mode and the cutoff frequency TE_{01} mode, that is, 13.1 GHz to 14.76 GHz. Besides, in this frequency range, the TE_{10} mode will propagate and should be suppressed.

Observing Figure 1, the 75-Ω coplanar waveguide and coplanar waveguide to slotline relay are packaged in a $10.16\,\text{mm} \times 8.0899\,\text{mm}$ ($H_a \times H_b$) metal shell to ensure that no rectangular waveguide mode is generated within the design frequency band and to shield interference from various external factors. The planar circuit is placed in the middle of the z-axis of the metal shell, resulting in the metal shell being divided into two $5.08\,\text{mm} \times 8.0899\,\text{mm}$ rectangles. Since the coplanar waveguide has odd- and even-modes, we use two air-bridges to suppress the odd-mode of the coplanar waveguide (coupled slotline mode) so that the feed end retains only the even-mode (coplanar waveguide mode). The terminal structure is a WR-90 rectangular waveguide with a short-circuited waveguide at

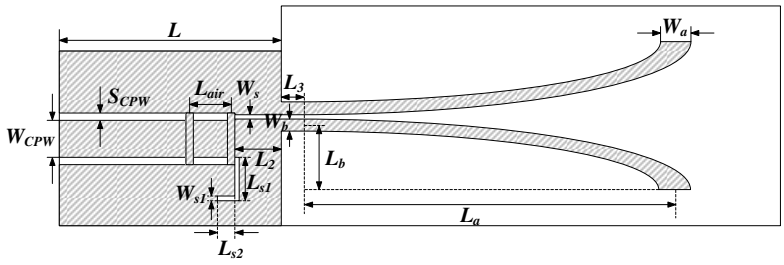

FIGURE 2. The planar circuit of the coplanar waveguide-to-rectangular waveguide TE_{20} mode transition using the antisymmetric tapered probe.

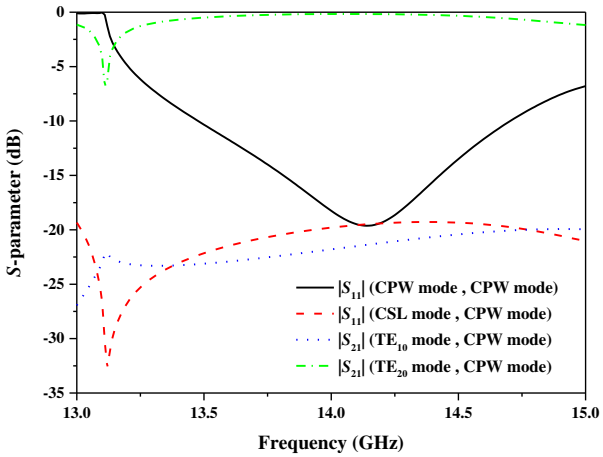

FIGURE 3. The frequency response of the S-parameters of the coplanar waveguide-to-rectangular waveguide TE_{20} mode transition using the antisymmetric tapered probe.

a distance D from the planar circuit. The distance D was designed to be approximately half the wavelength of the TE_{10} mode of the rectangular waveguide (about 12 mm at 14.1 GHz), which can well suppress the TE_{10} mode. Finally, the distance D was selected as 9.779 mm.

2.2. Circuit Analysis

First, TXLine is used to calculate dimensions of the 75-Ω coplanar waveguide, and the values of the dimensions are $W_{CPW} = 1.7272$ mm and $S_{CPW} = 0.3429$ mm. In addition, two air-bridges are used to suppress the coplanar waveguide odd-mode. The height and width of the air-bridges are 0.4 mm and 0.3 mm, respectively, and the distance L_{air} between the two air-bridges is 1.9 mm. The length of the short-circuited slotline is a quarter wavelength of 2.8 mm, so L_{S1} is chosen to be 2 mm and L_{S2} to be 0.8 mm, making its total length 2.8 mm. Its slot width W_{S1} is chosen as thin as the fabrication tolerance permits, so W_{S1} is 0.2 mm. The length of the antisymmetric tapered probe needs to be one wavelength in order to match the field pattern of the rectangular waveguide TE_{20} mode. Therefore, by fixing $L_b = 3$ mm and $W_a = 1.4$ mm, the length of the antisymmetric tapered probe is chosen as one wavelength of $L_a = 17.5$ mm. Then, the values of L_2, L_3, W_S, and W_b are adjusted to achieve impedance matching, and the dimensions are $L_2 = 2.16$ mm, $L_3 = 0.5$ mm, $W_S = 0.2032$ mm, and $W_b = 0.6$ mm, completing the overall coplanar waveguide-to-rectangular waveguide TE_{20} mode transition. The dimensions are summarized in Table 1. Next, Ansoft HFSS is used to simulate the coplanar waveguide-to-rectangular waveguide TE_{20} mode transition using the antisymmetric tapered probe in Figure 1. During the simulation, coplanar waveguide (CPW) mode and coupled slotline (CSL) mode are excited at the coplanar waveguide port, while the TE_{10} mode and TE_{20} mode are excited at the rectangular waveguide port. The frequency response of its S-parameters is shown in Figure 3. From the figure, the −10-dB bandwidth of the coplanar waveguide mode reflection coefficient covers 13.48 GHz to 14.7 GHz, and in this frequency band, the transmission coefficient of the rectangular waveguide TE_{10} mode is almost less than −20 dB, and the reflection coefficient of the coupled slot mode is less than −19 dB. The transmission coefficient of the TE_{20} mode is nearly 0 dB.

TABLE 1. The dimensions of the coplanar waveguide-to-rectangular waveguide TE_{20} mode transition using the antisymmetric tapered probe.

L	L_2	L_3	L_{s1}	L_{s2}	L_a	L_b	L_{air}
10.16	2.16	0.5	2	0.8	17.5	3	1.9
W_s	W_{s1}	W_a	W_b	W_{CPW}	S_{CPW}	D	Unit
0.2032	0.2	1.4	0.6	1.7272	0.3429	9.779	mm

FIGURE 4. The back-to-back photograph of the coplanar waveguide-to-rectangular waveguide TE_{20} mode transition using the antisymmetric tapered probe.

2.3. Verification

In order to verify the correctness of the simulation results, two of coplanar waveguide-to-rectangular waveguide TE_{20} mode transition using the antisymmetric tapered probe are connected back-to-back and fabricated as shown in Figure 4. Agilent

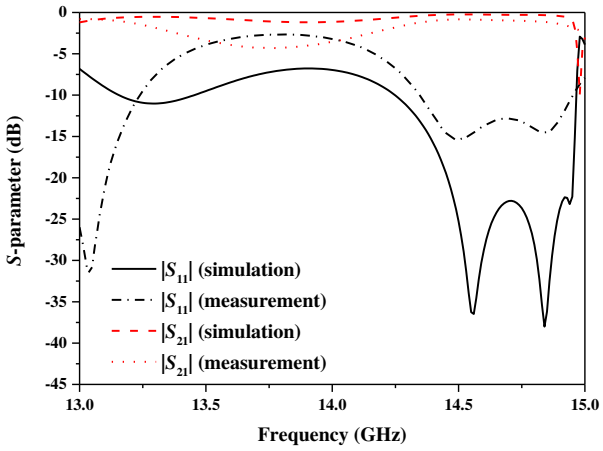

FIGURE 5. The comparison between the simulated and measured frequency responses of the S-parameters of the coplanar waveguide-to-rectangular waveguide TE_{20} mode transition using the antisymmetric tapered probe.

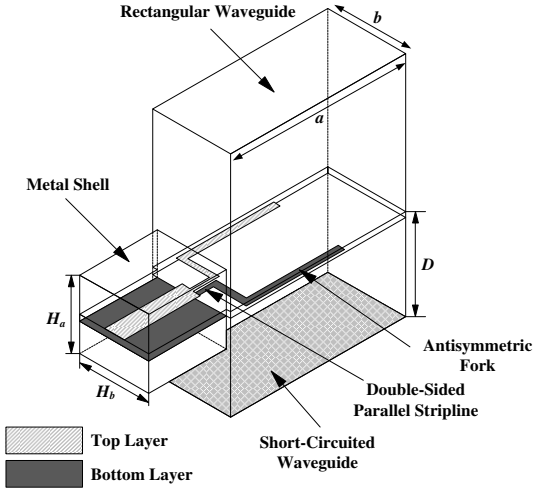

FIGURE 6. The schematic view of the microstrip line-to-rectangular waveguide TE_{20} mode transition using the antisymmetric fork.

N4433A ECal calibration kit is applied, and Agilent N5242A PNA is used to measure S-parameters. The comparison of the simulated and measured S-parameters of the back-to-back coplanar waveguide-to-rectangular waveguide TE_{20} mode transition using the antisymmetric tapered probe is shown in Figure 5. From Figure 5, the curve trends of the simulation and measurement results are similar, but there is a gap in the level. The low-frequency resonance is slightly offset, mainly due to the influence of the welding effect.

3. MICROSTRIP LINE-TO-RECTANGULAR WAVEGUIDE TE_{20} MODE TRANSITION USING ANTISYMMETRIC FORK

3.1. Topology

The schematic view of the microstrip line-to-rectangular waveguide TE_{20} mode transition using an antisymmetric fork is shown in Figure 6, and its planar circuit is shown in Figure 7.

The substrate used for the planar circuit is Rogers®RO5880, with a dielectric constant of 2.2, a tangent loss of 0.0009, and a substrate thickness of 0.8 mm. From Figure 7, the front end is a 50-Ω microstrip line feed; the middle is a double-sided parallel stripline, which is used to achieve impedance matching; the end is an antisymmetric fork, which gradually matches the field pattern to the rectangular waveguide TE_{20} mode. The rectangular waveguide used is WR-90 ($a = 22.86\,\text{mm} \times b = 10.16\,\text{mm}$), and its operating frequency band is between the TE_{20} cutoff frequency and TE_{01} cutoff frequency of WR-90, that is, 13.1 GHz to 14.76 GHz.

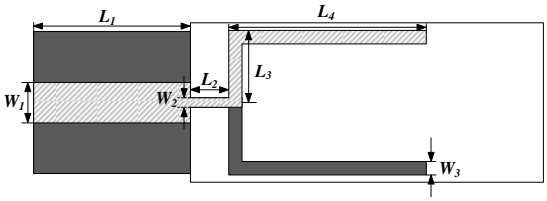

FIGURE 7. The planar circuit of the microstrip line-to-rectangular waveguide TE_{20} mode transition using the antisymmetric fork.

Reexamining Figure 6, the 50-Ω microstrip line feed is encapsulated by a metal shell with $H_a = 9\,\text{mm} \times H_b = 9\,\text{mm}$. In addition to resisting external interference, this metal shell can also keep the pure microstrip line mode inside the metal shell without generating any waveguide modes within the designed frequency band. The planar circuit is placed in the middle of the metal shell, and the height from the back short-circuited waveguide is D. The value of D is chosen to be half the wavelength of the rectangular waveguide TE_{10} mode (about 12 mm at 14.1 GHz) so that the TE_{10} mode can be suppressed.

TABLE 2. The dimensions of the microstrip line-to-rectangular waveguide TE_{20} mode transition using the antisymmetric fork.

L_1	L_2	L_3	L_4	D	W_1	W_2	W_3	Unit
10.16	2.5	4.6	12.8	12	2.5	0.6	0.8	mm

3.2. Circuit Analysis

First, TXLine is used to calculate the dimension of the 50-Ω microstrip line, and the width $W = 2.5\,\text{mm}$. By fixing the width of the antisymmetric fork $W_3 = 0.8\,\text{mm}$, L_3 is chosen as 4.6 mm, and L_4 is chosen as 12.8 mm so that the sum of them is one wavelength. Then by adjusting the values of L_2 and W_2 for impedance matching, dimensions of the double-sided parallel stripline are length $L_2 = 2.5\,\text{mm}$ and width $W_2 = 0.6\,\text{mm}$. The dimensions are summarized in Table 2. Then, Ansoft HFSS is used to simulate the structure of Figure 6. During the simulation, the microstrip line (MSL) mode is excited at the microstrip line port, while the TE_{10} mode and TE_{20} mode are excited at the rectangular waveguide port. The frequency response of its S-parameters is shown in Figure 8. From the figure, the frequencies where the microstrip line mode reflection coefficient is less than $-10\,\text{dB}$ range from 13.34 GHz to 15 GHz. In addition, within this frequency band, the transmission coefficient of the rectangular waveguide TE_{10} mode is less than $-20\,\text{dB}$. The transmission coefficient of the TE_{20} mode is nearly 0 dB.

TABLE 3. Comparison of the performance of the high-order mode rectangular waveguide transitions.

Transition Type	Waveguide Mode	Frequency Band	Insertion Loss (dB)	Length (mm)
Rectangular Waveguide Bend [14]	TE_{20}	7.98–9.07 GHz	−0.45	149
Cylindrical Waveguide [15]	TE_{13}	95–105 GHz	−5	31.63
Cylindrical Waveguide [16]	TE_{01}	46–51.4 GHz	−3	31.63
Fin-line [17]	TE_{20}	14–14.5 GHz	−0.9	N. A.
Antisymmetric Tapered Probe	TE_{20}	13.48–14.7 GHz	−0.59	18.7
Antisymmetric Fork	TE_{20}	13.34–15 GHz	−0.5	15.3

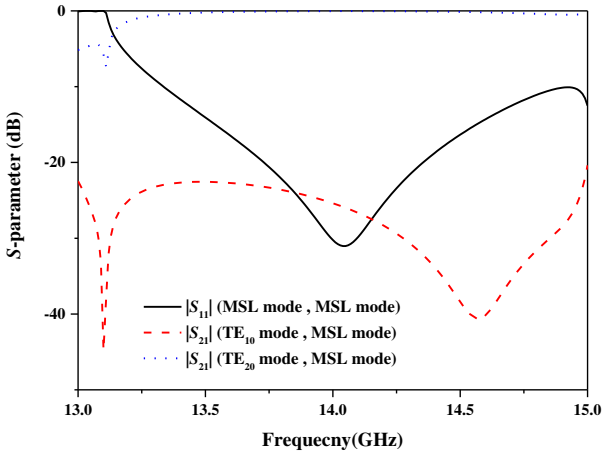

FIGURE 8. The frequency response of the S-parameters of the microstrip line-to-rectangular waveguide TE_{20} mode transition using the antisymmetric fork.

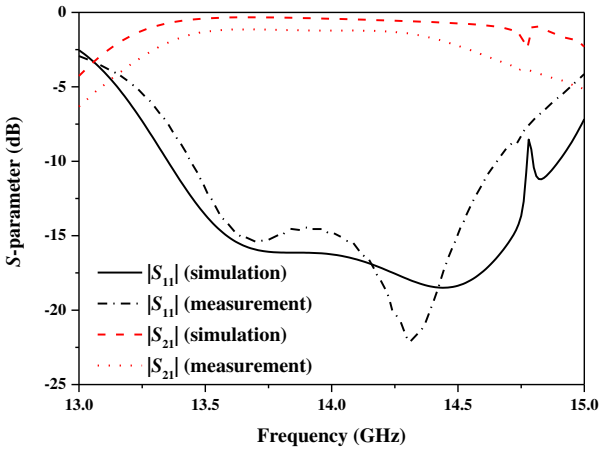

FIGURE 10. The comparison between the simulated and measured frequency responses of the S-parameters of the microstrip line-to-rectangular waveguide TE_{20} mode transition using the antisymmetric fork.

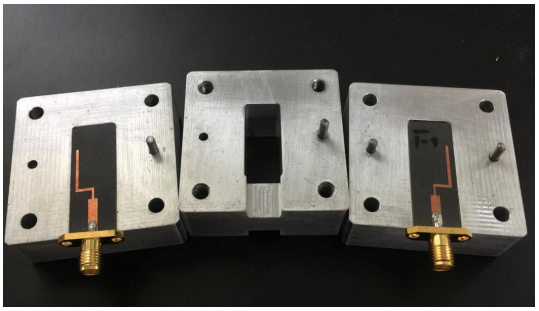

FIGURE 9. The back-to-back photograph of the microstrip line-to-rectangular waveguide TE_{20} mode transition using the antisymmetric fork.

3.3. Verification

In order to verify the accuracy of the transition design, two of microstrip line-to-rectangular waveguide TE_{20} mode transition using an antisymmetric fork are back-to-back connected and fabricated as shown in Figure 9. The comparison of the simulated and measured S-parameters of the back-to-back microstrip line-to-rectangular waveguide TE_{20} mode transition using the antisymmetric fork is shown in Figure 10. From Figure 10, it can be seen that the curve trends of the simulation and measurement are quite close, except that the resonance frequency point is slightly offset, and the level is not quite correct, mainly due to the influence of the welding effect.

4. CONCLUSION

In this paper, a coplanar waveguide-to-rectangular waveguide TE_{20} mode transition using the antisymmetric tapered probe is presented. The bandwidth of the −10 dB reflection coefficient of the coplanar waveguide mode covers 13.48 GHz to 14.7 GHz, and in this frequency band, the transmission coefficient of the TE_{10} mode is less than −20 dB, and the reflection coefficient of the coupled slotline mode is less than −19 dB. The transmission coefficient of the TE_{20} mode is nearly 0 dB. In addition, the microstrip line-to-rectangular waveguide TE_{20} mode transition using the antisymmetric fork has a −10-dB reflection coefficient of the microstrip line mode from 13.34 GHz to 15 GHz, and in this frequency band, the transmission coefficient of the rectangular waveguide TE_{10} mo is less than −20 dB. The transmission coefficient of the TE_{20} mode is nearly 0 dB. Two back-to-back transitions are fabricated and measured, where the simulation results agree well with the measurement ones. Table 3 summarizes the performance of the high-order mode rectangular waveguide transitions. As can be seen from Table 3, since the proposed transitions use antisymmetric probes for feeding, the transition volume can be substantially reduced.

ACKNOWLEDGEMENT

This work was supported in part by the National Science and Technology Council, Taiwan, under Grant NSTC 114-2221-E-011-075. The authors would like to thank Wireless Communications & Applied Electromagnetic LAB, National Taiwan University of Science and Technology, for providing the simulation environment of Ansoft®HFSS V.13 and the measurement instruments.

REFERENCES

[1] Ponchak, G. E. and R. N. Simons, "A new rectangular waveguide to coplanar waveguide transition," in *IEEE International Digest on Microwave Symposium*, Vol. 1, 491–492, Dallas, TX, USA, May 1990.

[2] Shireen, R., S. Shi, P. Yao, C. A. Schuetz, J. Macario, and D. W. Prather, "CPW to rectangular waveguide transition on an $LiNbO_3$ substrate," *IEEE Transactions on Microwave Theory and Techniques*, Vol. 57, No. 6, 1494–1499, Jun. 2009.

[3] Fang, R.-Y., C.-T. Wang, and C.-L. Wang, "A direct CPW-to-rectangular waveguide transition using a dipole slot antenna," in *2009 European Microwave Conference (EuMC)*, 157–160, Rome, Italy, 2009.

[4] Dong, Y., T. K. Johansen, V. Zhurbenko, and P. J. Hanberg, "Rectangular waveguide-to-coplanar waveguide transitions at U-band using *E*-plane probe and wire bonding," in *2016 46th European Microwave Conference (EuMC)*, 5–8, London, UK, Oct. 2016.

[5] Mottonen, V. S., "Wideband coplanar waveguide-to-rectangular waveguide transition using fin-line taper," *IEEE Microwave and Wireless Components Letters*, Vol. 15, No. 2, 119–121, Feb. 2005.

[6] Lin, T.-H. and R.-B. Wu, "CPW to waveguide transition with tapered slotline probe," *IEEE Microwave and Wireless Components Letters*, Vol. 11, No. 7, 314–316, Jul. 2001.

[7] Mottonen, V. S. and A. V. Raisanen, "Novel wide-band coplanar waveguide-to-rectangular waveguide transition," *IEEE Transactions on Microwave Theory and Techniques*, Vol. 52, No. 8, 1836–1842, Aug. 2004.

[8] Fang, R.-Y. and C.-L. Wang, "Miniaturized coplanar waveguide to rectangular waveguide transition using inductance-compensated slotline," *IEEE Transactions on Components, Packaging and Manufacturing Technology*, Vol. 2, No. 10, 1666–1671, Oct. 2012.

[9] Wang, S.-H., C.-C. Chang, Y.-C. Lee, and C.-L. Wang, "Compact and broadband CPW-to-RWG transition using stub resonators," *IEEE Transactions on Microwave Theory and Techniques*, Vol. 64, No. 10, 3198–3207, Oct. 2016.

[10] Yuan, B. and Z. Yu, "A wideband high-gain LTCC cavity antenna fed by TE_{20} mode substrate integrated waveguide for W-band applications," in *2022 IEEE MTT-S International Microwave Workshop Series on Advanced Materials and Processes for RF and THz Applications (IMWS-AMP)*, 1–3, Guangzhou, China, 2022.

[11] Chairi, Y., S. Abedrrabba, R. Allanic, A.-C. Amiaud, A. E. Oualkadi, C. Quendo, T. Merlet, K. Reklaoui, and T. L. Gouguec, "Design of a slotted waveguide antenna based on TE_{20} mode in ku-band suitable for direct metal laser sintering," *Electronics*, Vol. 11, No. 13, 2079, 2022.

[12] Tang, H., C. Tong, J.-X. Chen, C. Shao, W. Qin, and W. Yang, "Differentially SIW TE20-mode fed substrate integrated filtering dielectric resonator antenna for 5G millimeter wave application," in *2019 IEEE International Conference on Computational Electromagnetics (ICCEM)*, 1–3, Shanghai, China, 2019.

[13] Adhikary, M., A. Sarkar, A. Sharma, A. Biswas, and M. J. Akhtar, "TE_{20} mode air filled SIW based balun bandpass filter," in *2018 International Symposium on Antennas and Propagation (ISAP)*, 1–2, Busan, Korea (South), 2018.

[14] Zhang, Q., C.-W. Yuan, and L. Liu, "Theoretical design and analysis for TE_{20}-TE_{10} rectangular waveguide mode converters," *IEEE Transactions on Microwave Theory and Techniques*, Vol. 60, No. 4, 1018–1026, Apr. 2012.

[15] Liu, G., Y. Wang, Y. Pu, J. Wang, R. Yan, Y. Luo, and S. Wang, "A millimeter wave high-order TE_{13} mode converter," *IEEE Transactions on Electron Devices*, Vol. 63, No. 7, 2907–2911, Jul. 2016.

[16] Liu, G., Y. Wang, Y. Pu, and Y. Luo, "Design and microwave measurement of a novel compact $TE_{0n}/TE_{1n'}$-mode converter," *IEEE Transactions on Microwave Theory and Techniques*, Vol. 64, No. 12, 4108–4116, Dec. 2016.

[17] Martinez, R., M. Belaid, Z. Ouardirhi, J.-J. Laurin, and K. Wu, "Concept of a quasi-optic power amplifier utilising a new converter of mode TE_{10} to TE_{20}," in *CCECE 2003 — Canadian Conference on Electrical and Computer Engineering. Toward a Caring and Humane Technology (Cat. No.03CH37436)*, Vol. 1, 565–568, Montreal, QC, Canada, May 2003.